Online ISSN 1848-3380, Print ISSN 0005-1144
ATKAFF 56(2), 149–163(2015)

Junyi Liang, Jianlong Zhang, Hu Zhang, Chengliang Yin

Fuzzy Energy Management Optimization for a Parallel Hybrid Electric Vehicle using Chaotic Non-dominated sorting Genetic Algorithm

DOI 10.7305/automatika.2015.07.714
UDK 629.331-025.26:004.421.2

Original scientific paper

This paper presented a parallel hybrid electric vehicle (HEV) equipped with a hybrid energy storage system. To handle complex energy flow in the powertrain system of this HEV, a fuzzy-based energy management strategy was established. A chaotic multi-objective genetic algorithm, which optimizes the parameters of fuzzy membership functions, was also proposed to improve fuel economy and HC, CO, and NOx emissions. The main target of this algorithm is to escape from local optima and obtain high quality trade-off solutions. Chaotic initialization operator, chaotic crossover and mutation operators, chaotic disturbance operator, and chaotic local search operator were integrated into non-dominated sorting genetic algorithm II (NSGA-II) to form this new algorithm named chaotic NSGA-II (C-NSGA-II). Simulation results and comparisons demonstrated that chaotic operators can enhance searching ability for optimal solutions. In conclusion, C-NSGA-II is suitable for solving HEV energy management optimization problem.

Key words: Chaotic operator, Fuzzy logic, Hybrid electric vehicle, Multi-objective optimization, NSGA-II

Neizrazita strategija optimizacije potrošnje energije za paralelno hibridno električno vozilo korištenjem kaotičnog nedominirajućeg genetskog algoritma sortiranja. Ovaj rad prikazuje paralelno hibridno električno vozilo (HEV) opremljeno hibridnim spremnikom energije. Kako bi se omogućila funkcionalnost pogonskog sklopa ovakvog HEV-a korištena je strategija raspolaganja energijom zasnovana na neizrazitoj logici. Također, prikazan je više kriterijski genetski algoritam kaosa za optimiranje parametara neizrazite funkcije povezanih s ekonomskim pokazateljem te pokazateljima emisije HC-a, CO-a i NOx-a. Osnovni cilj algoritma je omogućiti izlazak iz lokalnih optimuma i uspostavljanjem kompromisa omogućiti dosezanje boljih rješenja. Kaotični inicijalizacijski operator, kaotično križanje i operator mutacije, kaotični operator poremećaja i kaotični operator lokalnog pretraživanje uključeni su u nedominirajući genetski algoritam sortiranja II (NSGA-II) u svrhu formulacije novog problema nazvanog kaotični NSGA-II (C-NSGA-II). Simulacijski rezultati i usporedbe prikazuju kako kaotični operator može povećati uspješnost traženja optimalnog rješenja. Zaključno, C-NSGA-II je primjeren za rješavanje problema raspolaganja energijom u HEV-u.

Ključne riječi: operator kaosa, neizrazita logika, hibridna električna vozila, više kriterijska optimizacija, NSGA-II

1 INTRODUCTION

With the increase of air pollution and energy consumption, energy conservation and environment protection have become major issues in the automotive industry [1–2]. Unlike conventional internal combustion engine (ICE) vehicles, hybrid electric vehicles (HEVs) can improve fuel economy and reduce exhaust emissions [3]. Combining ICE and an electric motor (EM) in an HEV powertrain system provides EM assistance and ensures that the ICE functions more effectively, thereby improving fuel economy [4].

However, because of HEV's complex powertrain system, an effective energy management strategy (EMS) must be explored to meet its control requirement. Fuzzy logic control has been widely used in different industries [5–7]. In recent decades, some researchers introduced fuzzy logic control in developing EMS for HEV [8–11]. Fuzzy logic control methods have been effectively adopted in its control domain. Nevertheless, membership functions (MFs) and fuzzy rules are normally designed based on engineering intuition, and achieving global optimization in such a way is difficult [12]. Thus, an appropriate optimization algorithm should be used to improve the performance of fuzzy logic controllers (FLCs).

In general, many researchers attempted to optimize fuel economy of HEV as a singular objective [13–15]. Other researchers attempt to optimize more objectives such as fuel economy and emissions, which are actually conflicting. Traditionally, a multi-objective optimization problem (MOP) is converted into a single-objective optimization problem by assigning weight values to each optimization objective [16–17]. However, allocating suitable weight values is difficult, especially when the objectives are conflicting. Thus, the traditional method is intrinsically limited when exploring the real trade-off relationship between objectives.

In this paper, we attempt to handle a MOP in the HEV domain: improving fuel economy and reducing hydrocarbon (HC), carbon monoxide (CO), and nitrous oxide (NOx) emissions. The four objectives are conflicting in some cases [12,18]. The challenge for the control strategy is to simultaneously balance these objectives for good fuel economy and low emissions. No fixed evaluation standard has been established to determine the best solution. Therefore, good trade-off solutions are considered optima in view of multi-objective optimization [19].

Non-dominated sorting genetic algorithm II (NSGA-II) is an efficient evolutionary algorithm that can solve a multi-objective problem [20]. NSGA-II was presented by Deb in 2002 and has been successfully applied to optimize reactive power dispatch problems [21], automatic test task scheduling problems [22], propulsion system of marine vessels [23], and other optimization problems. This method can effectively obtain improved spreading solutions. However, because the amount of new individuals created may be limited, it may lack diversity and be trapped in local optima [24]. In addition, HEV is a complex mechanical and electrical combination system. Therefore, the optimization for an HEV's EMS should be carefully chosen and designed.

As a complex nonlinear dynamics behavior, chaos is a general phenomenon in nature. It has several specific characteristics, such as stochasticity and ergodicity [25]. As a result of these properties, chaos search is more capable of hill climbing and escaping local optima than random search. Thus, some researchers have combined chaos search with optimization algorithms to obtain better performance. For instance, Guo et al. [26] applied chaos optimization in the initial population and final optima solution local search. Mahdiyeh [27] introduced chaotic sequence into particle swarm optimization to improve global searching capability and escape premature convergence to local minima for a power system stabilizer design. Although researchers have studied approaches that combined chaos with evolutionary algorithms in various fields, the research on combing chaotic operators with NSGA-II has not been well addressed [22, 24, 26] and will be explored in detail in this study. Meanwhile, it is also the first time that adopting the NSGA-II combined with chaotic operators in the domain of HEV as in this study.

In this paper, we introduce chaotic initialization operator, chaotic crossover and mutation operators, chaotic disturbance operator, and chaotic local search operator into NSGA-II to enhance the performance of the original algorithm. The modified chaotic NSGA-II (C-NSGA-II) is used to find better trade-off solutions for fuel economy and emissions for a parallel HEV equipped with a hybrid energy storage system (HESS). A fuzzy-based EMS was previously established for this HEV. Thus, the C-NSGA-II can be used to search the best MF parameters in FLCs. The remainder of this paper is organized as follows: Section 2 describes the powertrain architecture of the target HEV, Section 3 presents the fuzzy EMS of this HEV, Section 4 introduces the basic concepts of MOP, and Section 5 presents the MOP for the target HEV, including problem formulation, description of objectives, and chromosome coding. Section 6 describes C-NSGA-II in detail, while Section 7 presents simulation results and performance comparison. Section 8 presents the conclusion and future research directions.

2 POWERTRAIN ARCHITECTURE AND ENERGY MANAGEMENT STRATEGY

The parallel hybrid electric vehicle (HEV) studied in this paper is mainly aimed at mid-range and low-end vehicle markets. The kinetic performance of this parallel HEV is shown in Table 1 [28].

Table 1. Kinetic performance of target parallel HEV

Item	Value
Maximum velocity (km/h)	≥ 80
0 km/h to 50 km/h acceleration time (s)	≤ 20
Gradeability (%)	≥ 20

The powertrain architecture of this HEV is presented in Fig. 1. A double-cylinder internal combustion engine (ICE) with small displacement is integrated at the front drive axle. A small permanent magnet brushless direct current electric motor (EM) is used at the rear drive axle. The energy storage system (ESS) used in this HEV is a battery/ultracapacitor (UC)-based hybrid energy storage system (HESS). The HESS is composed of a battery pack, a UC pack, and a bi-directional DC/DC converter. The UC pack connects with the battery pack through the bi-directional DC/DC converter.

In practice, battery-only ESSs have been widely adopted in commercially available HEVs. However, the relatively low power density of batteries hinders them from

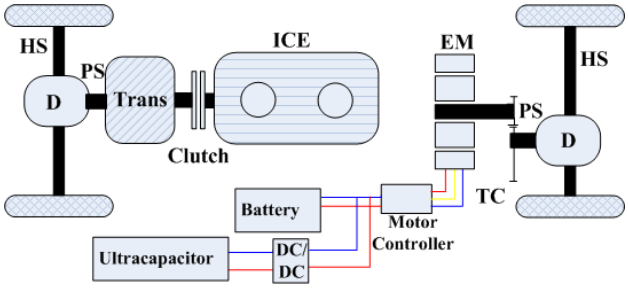

Fig. 1. Architecture of parallel HEV's powertrain

performing well to meet the high electric power requirements of HEVs in some modes, such as pure electric acceleration and regenerative braking (RB) [29]. UCs have lower energy density and higher power density than batteries. Their specific features enable energy to be stored and released without chemical reaction. Thus, the energy can be absorbed and released immediately with low losses. Therefore, UC is capable of meeting the instantaneous high power demand of EM. Based on the different features of batteries and UCs, a battery/UC-based HESS can be constructed. In HESS, the battery meets only the average electrical power requirement during HEV driving. On the other hand, UC is used to compensate for fluctuations in electrical power demand. The combination of the two electrical sources can mitigate battery workload, which will improve the working efficiency of the battery and extend its life expectancy. Moreover, the high power density of UCs makes HESS more effective in absorbing regenerative power during vehicle braking. Thus, HESS can be used to obtain better energy efficiency than traditional ESS. The specifications of the parallel HEV are listed in Table 2.

Table 2. Specifications of the parallel HEV

Vehicle and components	Parameter	Value
Vehicle	Curb/gross weight (kg)	850/1150
	Tire rolling radius (m)	0.28
	Frontal area (m^2)	1.91
	Aerodynamic drag coefficient	0.34
	Rolling resistance coefficient	0.009
ICE	Idle/maximum speed (rpm)	1400/8000
	Maximum torque (Nm)	18.7/5500
	Maximum power (kW)	12.7/7000
	Displacement (l)	0.25
Electric motor	Peak power (kW)	14
	Continuous power (kW)	7
	Peak torque (Nm)	70
LiFePO4 Battery	Capacity (Ah)	40
	Equivalent series resistance (Ω)	0.052
	Nominal operating voltage (V)	72
Ultra capacitor	Capacitance (F)	165
	Nominal operating voltage (V)	48.6
	Emax (Wh/kg)	3.81
	Pmax (W/kg)	7900

3 ENERGY MANAGEMENT STRATEGY

To address the complex power distribution in HEV, a fuzzy-based EMS is developed. HEV may run in several modes, namely, pure electric mode (PEM), parallel mode (PM), and braking mode (BM). Mode selection is mainly based on pedal position and vehicle speed. If the accelerator pedal is pressed, HEV will run in PEM or PM. When the vehicle speed is higher than a threshold, PEM will change to PM, and ICE will start. Some constraints are in place to protect the battery and UC. When the battery's state of charge (BSOC) falls below 20% or the UC's state of charge (USOC) falls below 50%, the PEM mode will automatically change to PM. On the other hand, if the brake pedal is pressed, HEV will run in BM. As shown in Fig. 2, each mode has a related fuzzy logic controller (FLC) that handles power distribution. Three FLCs are used in this study, namely, PEM FLC, PM FLC, and regenerative braking (RB) FLC. The ICE torque, EM torque, battery power, and UC power can be assigned and sent to each corresponding HEV component by the EMS.

3.1 Pure Electric Mode Fuzzy Logic Controller

PEM FLC is specifically designed for electrical power distribution for HESS in the PEM. Figure 3 shows a block diagram of the PEM FLC. The inputs of this FLC are the P_EM (Required electrical power of EM based on the current driving power requirement and also the EM efficiency), BSOC, and USOC.

The output of PEM FLC is indicated as Pro_UC, which means the proportion of P_EM is supplied by the UC, while the rest of P_EM is supplied by the battery. The battery has the advantage in energy density, whereas the UC has the advantage in power density. Based on their different features, a proper PEM FLC is established. The battery provides total electrical power if USOC is low. Otherwise, P_EM is met by both battery and UC. The power distribution between the battery and UC is determined by their SOC status and operation power condition of EM. The rule

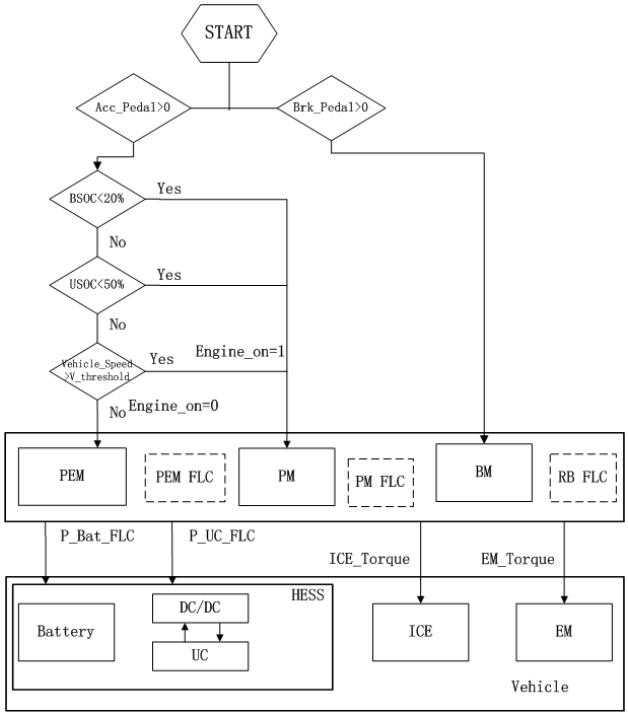

Fig. 2. EMS topology

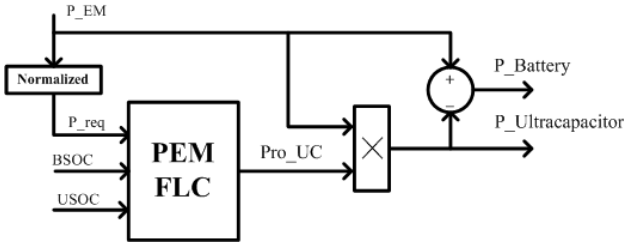

Fig. 3. Block diagram of PEM FLC

base of PEM FLC is shown in Fig. 4. The MFs of each input and output of this FLC and of two other FLCs are shown and discussed in Section 5.

3.2 Parallel Mode Fuzzy Logic Controller

PM is a "full" mode in which both ICE and EM to work together for this HEV. Figure 5 presents the block diagram of the proposed PM FLC, which has three inputs and one output. The inputs are ICE speed, accelerator pedal position (K), and BSOC. The output is the Tice which represents the torque percentage of the maximum engine torque at current rotational speed. Specifically, the value 0.5 of Tice indicates the highest efficiency operation torque of ICE, which will change according to ICE speed.

The energy stored in the battery is significantly larger than that in the UC. Therefore, PM FLC focuses on regulating the BSOC level by adjusting the ICE operation

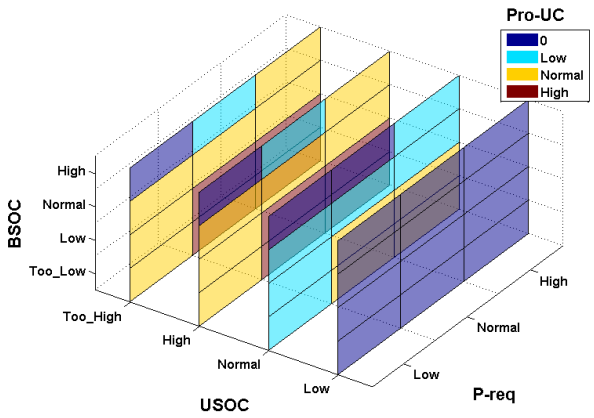

Fig. 4. Rule base of PEM FLC

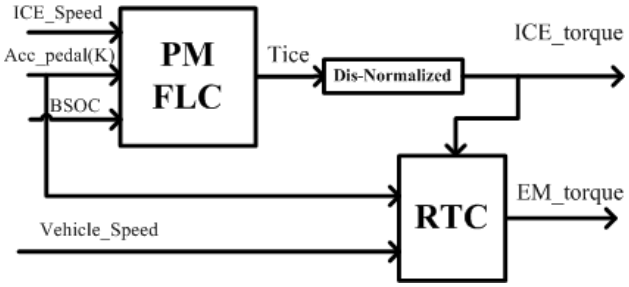

Fig. 5. Block diagram of PM FLC

torque. The PM FLC intends to control the ICE operating at a comparatively high efficiency. However, to maintain the BSOC at a normal range, the torque command of the ICE can be tuned. If the BSOC is high enough, the ICE power decreases and EM provides more power. If the BSOC is low, the ICE will output more power to charge the battery. Given that the PM FLC only distributes power between ICE and EM, power management of HESS requires cooperation among PM FLC and other FLCs. When PM FLC outputs a positive power command to EM, the HESS has to output power for EM-assisted driving. Then, the PEM FLC is called to distribute the output power between the battery and the UC. When the EM regenerates power to charge HESS, RB FLC (as presented in Section 3.3) meets the regenerative power distribution requirement. The rule base of PM FLC is presented in Fig. 6.

3.3 Regenerative Braking Fuzzy Logic Controller

RB FLC handles the regenerative braking condition. The block diagram of this FLC is shown in Fig. 7. The two inputs of RB FLC are BSOC and USOC, and the output is Pro_UC. RB FLC mainly distributes the regenerative power between the battery and the UC. With its high power

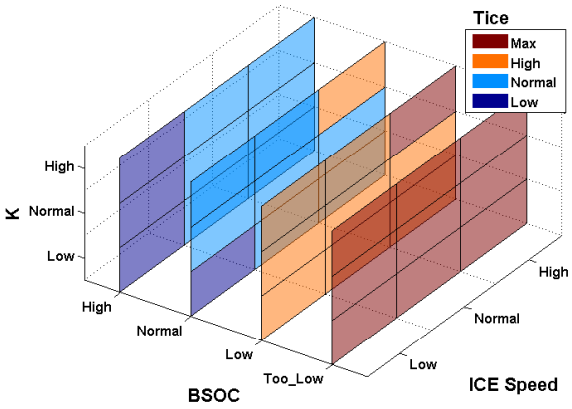

Fig. 6. Rule base of PM FLC

density and dynamic performance, UC should be charged first by the large current when HEV breaks in a hard transient state. When USOC is low, UC receives more RB power. When USOC is high, the battery acquires more RB power. Figure 8 shows the rule base of RB FLC.

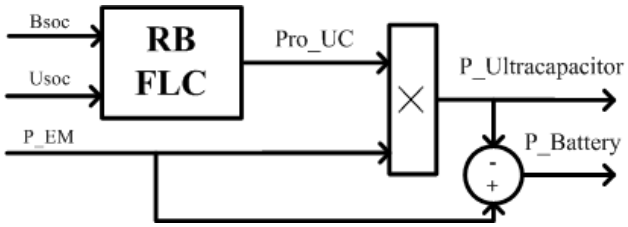

Fig. 7. Block diagram of RB FLC

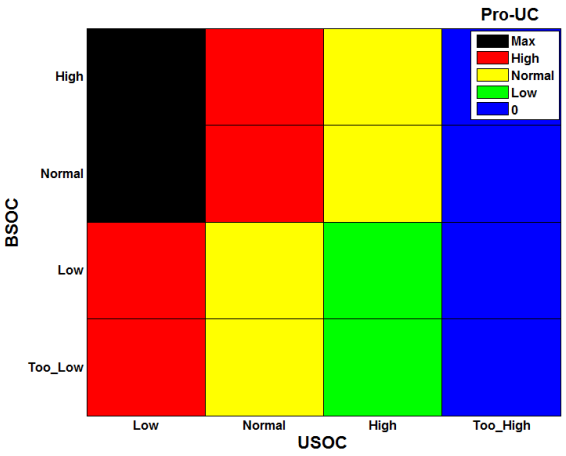

Fig. 8. Rule base of RB FLC

4 MULTI-OBJECTIVE OPTIMIZATION PROBLEM

This paper proposes a multi-objective optimization algorithm based on Non-dominated sorting genetic algorithm II (NSGA-II) and chaotic theory for fuzzy energy management optimization in HEV. Before explaining this algorithm in detail, the multi-objective optimization problem (MOP) should be introduced briefly [30].

An MOP can be described as follows:

$$\begin{aligned} &\text{minimise} \quad F(x) = \left(f_1(x), f_2(x), ..., f_M(x)\right)^T \\ &\text{subject to} \quad x \in \Omega \end{aligned} \tag{1}$$

where Ω is the decision (variable) space, $F : \Omega \to R^m$ consists of m real-valued objective functions, and R^m is called the objective space. Normally, the objectives in (1) are conflicting, and perhaps no x can simultaneously minimize all the objectives. However, trade-off solutions that attempt to balance different objectives can be obtained. The best solutions can be called *Pareto optimal set* and can be defined as follows [31]:

Definition 1 (Pareto dominance) *A feasible decision vector x_a is said to dominate another feasible vector x_b (denoted by $x_a \prec x_b$) if the following two conditions are satisfied:*

(i) x_a is no worse than x_b in all objectives

$$\forall i = 1, 2, \ldots, m \quad f_i(x_a) \leq f_i(x_b). \tag{2}$$

(ii) x_a is strictly better than x_b in at least one objective

$$\exists i = 1, 2, \ldots, m \quad f_i(x_a) \prec f_i(x_b). \tag{3}$$

If there is no solution x_a that dominates x_b then x_b is a Pareto optimal solution.

Definition 2 (Pareto Optimal Set) *For a given MOP, the Pareto optimal set, PS, is defined as*

$$PS := \{x \in F | \neg \exists x^* \in F, x^* \prec x\}. \tag{4}$$

Definition 3 (Pareto Front) *For a given MOP and Pareto optimal set, Pareto front, PF, is defined as*

$$PF := \{f(x) | x \in PS\}. \tag{5}$$

5 PROBLEM FORMULATION OF FUZZY ENERGY MANAGEMENT OPTIMIZATION

5.1 Formulation of tuning the FLCs as an optimization problem

The fuzzy logic controllers (FLCs) described in Section 3 were designed according to expert knowledge and intuition. Therefore, the original FLCs' parameters do not necessarily lead to an optimal result, and they need further optimization. The membership function (MF) parameters in

these FLCs can be tuned to find better solutions for HEV's fuel economy and emissions. In this study, we set four objectives that are equivalent fuel consumption (EFC) and the HC, CO, and NOx emissions from the target HEV over an entire Economic Commission of Europe (ECE) driving cycle, as shown in Fig.9.

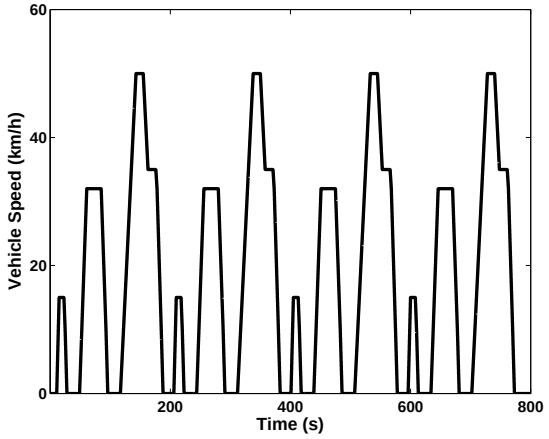

Fig. 9. Economic Commission of Europe driving cycle

During the driving, the HEV will not only consume the fuel by running ICE but also consume the electrical energy in HESS by using EM. Thus, the total energy consumption should include both the fuel consumption and the electrical energy consumption. Assuming the ICE can drive EM to generate power for charging HESS back to its initial electrical energy level, there is a relationship between the HESS's equivalent fuel consumption ($\mathrm{EFC}_{\mathrm{HESS}}$) and the HESS electrical energy consumption, as shown in equation (6) [28]:

$$\mathrm{EFC}_{\mathrm{HESS}} = \frac{3600 E_{\mathrm{HESS}}}{D_{\mathrm{f}} Q_{\mathrm{f}} \eta_{\mathrm{gen}}} \tag{6}$$

where E_{HESS} is the consumed HESS energy, D_{f} is the density of fuel, and Q_{f} is the low heat value of gasoline. The generator-set efficiency η_{gen} is assumed as 30% on average. The total EFC includes both actual fuel consumption and $\mathrm{EFC}_{\mathrm{HESS}}$.

These four objectives may be conflicting. Thus, minimizing all of them simultaneously could be difficult. However, their Pareto optimal sets can be found by using the C-NSGA-II. The objectives are as follows:

$$\begin{aligned} &\text{Objective functions (to be minimized):} \\ &f_1(Z) = \textstyle\int_0^{T_D} \mathrm{VFR}_{\mathrm{EFC}}\, dt \\ &f_2(Z) = \textstyle\int_0^{T_D} \mathrm{MFR}_{\mathrm{HC}}\, dt \\ &f_3(Z) = \textstyle\int_0^{T_D} \mathrm{MFR}_{\mathrm{CO}}\, dt \\ &f_4(Z) = \textstyle\int_0^{T_D} \mathrm{MFR}_{\mathrm{NOx}}\, dt \end{aligned} \tag{7}$$

where T_D is the time duration of the ECE driving cycle, and Z is a vector that contains all parameters that need to be tuned, VFR is the volume flow rate of EFC and MFR is the mass flow rate for three emissions: HC, CO and NOx.

5.2 Coding the parameters of MFs

In FLCs, the decision variables of MFs are critical issues for the optimization process. These variables are coded into chromosomes that evolved from C-NSGA-II. When the variable number increases, the length of the chromosome also increases. A lengthening chromosome will require a larger population size and more generations to achieve a satisfactory solution, which would increase the computational time cost. To address this difficulty, the minimum amounts of variables that can fully define MFs are used.

The default FLCs and their tunable MFs are shown in Fig. 10. A total of seven input or output variables are adopted in our three FLCs; these variables are ICE speed, K, BSOC, Tice, P_req, USOC, and Pro_UC. Triangular MFs and trapezoidal MFs are used in these variables.

To limit the number of variables that define MFs, several fixed values are chosen. As shown in Fig. 10(a), the center of the triangular MF "Normal" is fixed at 0.4 because it is the normalized highest efficiency speed region of the ICE. The inside corners of trapezoidal MFs "Low" and "High" are also fixed at 0.4 to guarantee adequate overlap of MFs. Three variables, namely, Z1, Z2, and Z3, are adopted in Fig. 10(a), and bounds of these variables are limited such that the corresponding MFs can remain compatible with the meaning of their labels. A symmetrical triangle pattern for the MF "Normal" to limit the numbers of variables in chromosome is adopted. Similar concepts are applied to other variables. K, Tice, P_req, Pro_UC have triangular MFs "Normal" which are all fixed at 0.5, and BSOC and USOC have their own particular "Normal" MF values. These values are 0.65 for BSOC and 0.75 for USOC, which originated from the highest and reasonable efficiency working region for battery and UC. As depicted in Fig. 10, 20 variables are coded into a chromosome by using real value coding scheme. A 21$^{\mathrm{st}}$ variable, Z21 is also used to decide the switching speed for mode switching from PEM to PM. According to the corresponding ICE working speed, we limit the Z21 that varies from 7.5 to 12 (km/h). Its default value is 10. The 21 variables are coded as follows:

$$Z = (Z1, Z2, ..., Z21)\,. \tag{8}$$

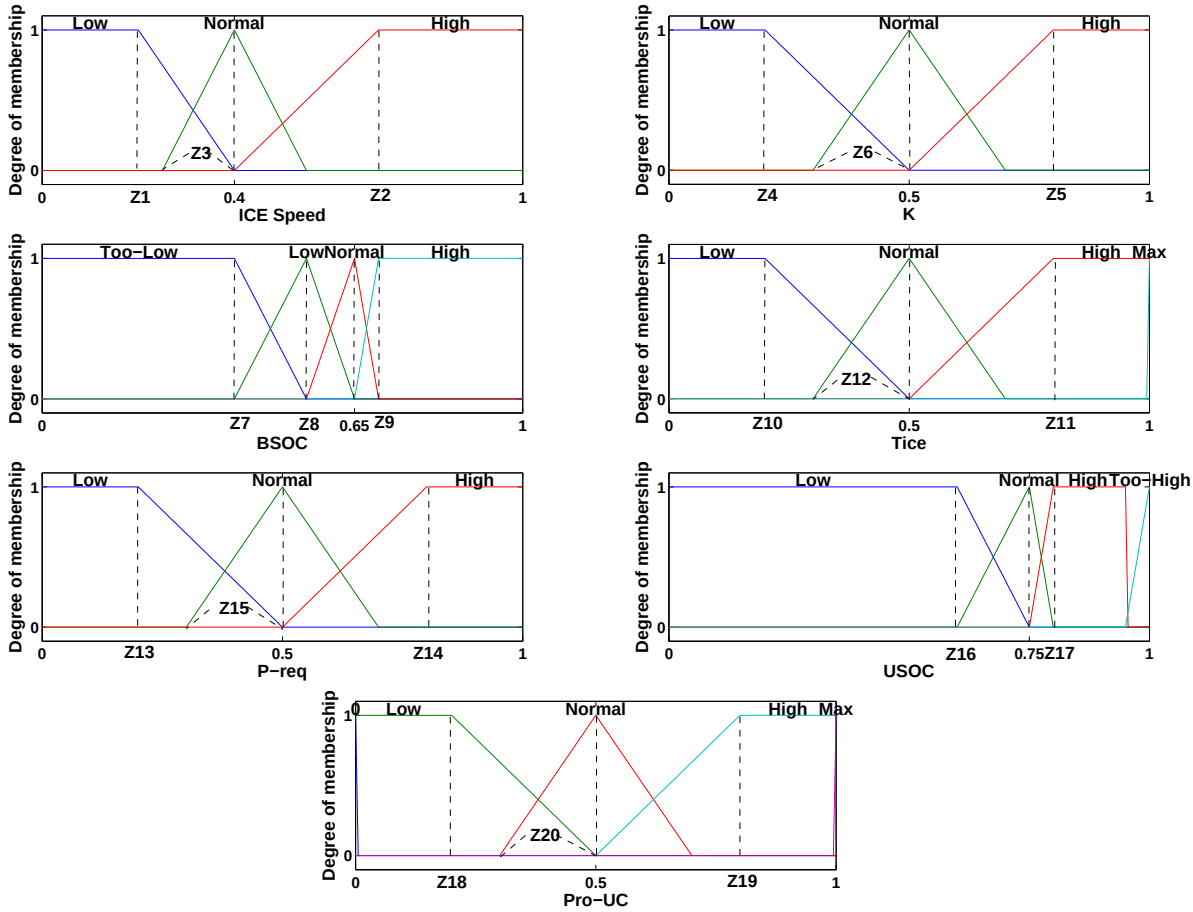

Fig. 10. Membership functions of three default FLCs (a) ICE Speed, (b) K, (c) BSOC, (d) Tice, (e) P_req, (f) USOC, (g) Pro_UC

Constraints of these variables are as follows:

$$\left(\begin{array}{l} 0 < Z1 < 0.4, 0.4 < Z2 < 1, 0 < Z3 < 0.4, \\ 0 < Z4 < 0.5, 0.5 < Z5 < 1, 0 < Z6 < 0.5, \\ 0.3 < Z7 < Z8 < 0.65, 0.65 < Z9 < 0.8, \\ 0 < Z10 < 0.5, 0.5 < Z11 < 1, 0 < Z12 < 0.5, \\ 0 < Z13 < 0.5, 0.5 < Z14 < 1, 0 < Z15 < 0.5, \\ 0.5 < Z16 < 0.75, 0.75 < Z17 < 1, \\ 0 < Z18 < 0.5, 0.5 < Z19 < 1, 0 < Z20 < 0.5, \\ 7.5 < Z21 < 12. \end{array}\right) \tag{9}$$

Thus, MOP in this study has four objectives and 21 variables. The C-NSGA-II that handles this MOP is presented in the next section in detail.

6 CHAOTIC NON-DOMINATED SORTING GENETIC ALGORITHM-II

In this study, we develop a hybrid evolutionary algorithm by combining the chaotic method and NSGA-II. In a chaotic system, a small change of the initial condition will lead to a completely different future behavior. These features of the chaotic system are called ergodic and stochastic [25]. As a result of these features, combining chaotic method and evolutionary algorithm will dictate some special properties such as increasing solutions' diversity and escaping from local optima [24].

We adopted a logistic map in this study, which is a one-dimensional chaotic map popularized by biologist Robert Mary in 1976 [32]. This map can be defined as follows [33]:

$$x_{i+1} = \mu x_i \left(1 - x_i\right), \quad x_i \in (0,1), \quad i = 1, 2, \ldots \tag{10}$$

where x_i is the value of chaotic variable x at the ith iteration, and μ is the so-called bifurcation parameter of the system ($\mu \in [0,4]$), which is equal to 4 in this study. The initial value of x_0 is generated randomly between 0 and 1, with $x_0 \notin \{0.25, 0.5, 0.75\}$.

The chaotic logistic map generates the chaotic sequences that are embedded in NSGA-II to form a new hybrid algorithm. However, the main framework of NSGA-II

is maintained, which is briefly introduced as follows [16, 20]:

(1) The parent population, including N individuals, is initialized, and this population is sorted based on the non-domination level.

(2) Crossover and mutation operators on the parent population are used to create an offspring population.

(3) The parent and offspring populations are combined, and all the individuals are ranked based on their non-domination level.

(4) The top N individuals are chosen as the new parent population, and the lower-ranking individuals are abandoned.

(5) Steps (2) to (4) are repeated until the stop criterion is satisfied.

As the iteration continues, the new individuals gradually move toward PS.

Based on the NSGA-II framework, some new chaotic operators are embedded into the former algorithm to improve performance. These operators are presented as follows:

A. Chaotic initialization operator

The initial population with N individuals is generated by using command "rand(·)" in the original NSGA-II. The chaotic logistic map is used instead for the generation of the initial population in this study. If j is the serial number of variables, then the chaotic variable x_i^j has to be transformed to the interval of the corresponding optimization variable Z_i^j, as shown in the following:

$$Z_i^j = a^j + \left(b^j - a^j\right) x_i^j. \tag{11}$$

where a^j and b^j are the lower and upper bounds of the optimization variable Z^j, respectively. Adopting the above method in 21 variables in N individuals generates the initial population.

B. Chaotic crossover and mutation operator

The original NSGA-II randomly generates a number rc to decide whether the crossover operation should be executed. If the $rc$is smaller than the crossover probabilityp_c, the simulated binary crossover (SBX) will be executed. We used another crossover operator called differential evolution (DE) [34]. The performances of the DE operator and SBX are compared; the former consistently outperformed the latter [35]. DE crossover operator goes through each parent of the population as the index primary parent, and for each primary parent it also chooses another three auxiliary parents which are randomly selected from the current population and mutually different and different from the index primary parent. By taking four (one primary and three auxiliary) parents DE crossover operator can create one offspring by using equation (12) [36]. The index primary parent is set as p_i, and the auxiliary parents are set as a_1, a_2 and a_3. The number of variables M in a chromosome is equal to 21 as described in section 5, and j_r is a random number (uniformly distributed) between 1 and M. DE operator uses two tuning parameters, namely, $F = 0.5$ and $CR = 0.9$. Here, u_j is a uniformly distributed random number in [0, 1], the offspring solution is os, and the subscript j denotes the j^{th} variable. Then, os is given as follows: cases

$$os_j = \begin{cases} (a_3)_j + CR((a_1)_j - (a_2)_j) & \text{if } u_j \prec F \text{ or } j = j_r \\ (p_i)_j & \text{otherwise} \end{cases} \tag{12}$$

Each offspring has a corresponding index primary parent. Thus, the size of offspring population is the same as that of the parent population.

The offspring is mutated before evaluation by using the polynomial mutation operator from the original NSGA-II. A randomly generated number rm is used to decide whether the mutation operation should be executed. If rm is smaller than the mutation probability p_m ($p_m = 0.2$ in this case), polynomial mutation will be applied. Here, x_j and $x_j^{'}$ are set as the value of variable j before and after the mutation, respectively. Meanwhile, r_j is set as a uniformly distributed random number in [0, 1] and $\eta_m = 20$ is the distribution index for mutation. Then, $x_j^{'}$ is given as follows:

$$\begin{aligned} \delta_q &= \begin{cases} (2r_j)^{1/(\eta_m+1)} - 1\,, & \text{if } r_j \prec 0.5 \\ 1 - (2 \times (1 - r_j))^{1/(\eta_m+1)}\,, & \text{otherwise} \end{cases} \\ x_j^{'} &= x_j + (b^j - a^j) \times \delta_q \end{aligned} \tag{13}$$

If $x_j^{'}$ is higher than the upper bound b^j or lower than the lower bound a^j, its value will be limited at the boundaries. Here, u_j and r_j are created by a chaotic logistic map according to (10) instead of through random generation "rand()".

C. Chaotic disturbance operator

As the iteration process continues, the original NSGA-II may lack diversity, and some solutions may be trapped in the local optima. To increase the diversity of solutions, chaotic disturbance operator is adopted in C-NSGA-II. At every generation, after the crossover and mutation operation on the parent population, chaotic new individuals of 10% of the parent population are created by chaotic logistic map as in equation (11). These new individuals are added to the evaluation and non-dominated ranked process. The N number individuals of the next new generation are selected from the parent population, offspring population, and chaotic new individuals. Thus, each generation population's diversity increases, and some local optima trapped situations can be avoided.

Table 3. Application of chaotic operators

Operators	NSGA-II	C-NSGA-II-1	C-NSGA-II-2
Chaotic initialization	×	✓	✓
Chaotic crossover	×	✓	✓
Chaotic mutation	×	✓	✓
Chaotic disturbance	×	×	✓
Chaotic local search	×	×	✓

D. Chaotic local search operator

One more chaotic operator remains for the C-NSGA-II. After selecting the new individuals for the next generation, chaotic local search (CLS) operator will be executed on the top 10% elite individuals. The basic idea of CLS is searching the hypercube neighborhood of elite individuals, which ensures that solutions can escape from local optima and that better individuals that move toward PS can be found [33]. For each elite individual, CLS solutions can be calculated by using the following equation:

$$x_c^j = x_e^j + \lambda_g \times (b^j - a^j) \times (2 \times L^k - 1). \qquad (14)$$

where L^k is the chaotic vector produced by logistic map. Twenty logistic map chaotic solutions from each elite individual are acquired at a time. The jth variable x_c^j in the newly created chaotic solution can be calculated from the original variable x_e^j and the variable boundary constraints are still efficient. Here, λ_g is set as 1/current generation. Thus, the neighborhood searching space will decrease as the generation increases. The 20 chaotic solutions are compared with the corresponding elite individual. If a better solution is found, the elite individual will be replaced. Searching the neighborhood of elite individuals can discover better solutions. Then, solutions of C-NSGA-II will move faster toward PS than the original NSGA-II.

7 SIMULATION RESULTS AND DISCUSSION

7.1 Simulation Environment and Performance Metrics

The performance of the proposed C-NSGA-II is compared with that of the original NSGA-II for the optimization of fuzzy logic controllers. To compare the efficiencies of different chaotic operators, two stages of C-NSGA-II are adopted, which are separately named C-NSGA-II-1 and C-NSGA-II-2. The application of the chaotic operators in different algorithms is detailed in Table 3.

For MOP, both convergence to $PS$and maintenance of solution diversity should be considered. Two metrics that refer to these two aspects are used.

1. Coverage of two sets [37]
   Let $X^{'}, X^{''} \subseteq X$ be two sets of non-dominated solutions. The function *C* maps the ordered pair $(X^{'}, X^{''})$ to the interval [0, 1]:

$$C(X^{'}, X^{''}) := \frac{|\{x^{''} \in X^{''}; \exists x^{'} \in X^{'} : x^{'} \geq x^{''}\}|}{|X^{''}|}. \qquad (15)$$

   The value $C(X^{'}, X^{''}) = 1$ means that all the solutions in $X^{''}$ are dominated or equal to solutions in $X^{'}$. By contrast, $C(X^{'}, X^{''}) = 0$ means no solution in $X^{''}$ is dominated or equal to solution in $X^{'}$. The value of $C(X^{'}, X^{''})$ is not necessarily equal to, $1 - C(X^{''}, X^{'})$. Thus, both $C(X^{'}, X^{''})$ and $C(X^{''}, X^{'})$ have to be considered.

2. Spacing [38]
   Metric spacing *S* is used to measure the range variance of neighboring vectors in the obtained solutions. It is defined as follows:

$$S = \sqrt{\frac{1}{|X'| - 1} \sum_{i=1}^{|X'|} (\bar{d} - d_i)^2} \qquad (16)$$

$$d_i = \min_j \left\{ \sum_{k=1}^{p} |f_k(x_i) - f_k(x_j)| \right\}; x_i, x_j \in X^{'} \qquad (17)$$

   where $i, j = 1, 2, ..., |X^{'}|$, $\bar{d}$ is the average value of all d_i, and p is the number of objective functions. A smaller value of spacing means that the solutions are more uniformly distributed.

Both NSGA-II and C-NSGA-II are implemented in M language in Matlab/Simulink environment. These algorithms can call the vehicle model established in Simulink [28] to run the ECE driving cycle and obtain the EFC and emission data as the objective values. We adopt N = 100 individuals to form the initial population and set the terminating condition as 50 generations. Any solution that can not satisfy the kinetic constraints of the target HEV will be eliminated and replaced by a chaotic-based new one. All simulations are executed in Matlab 7.12.0 (R2011a) on an Intel(R) Core(TM)2 T5450 1.66 GHz PC with 2.5 GB RAM.

7.2 Simulation Results

In this study, the four objectives are the accumulated output values of the target HEV model in an ECE driving cycle: EFC and HC, CO, and NOx emissions. Figure 11

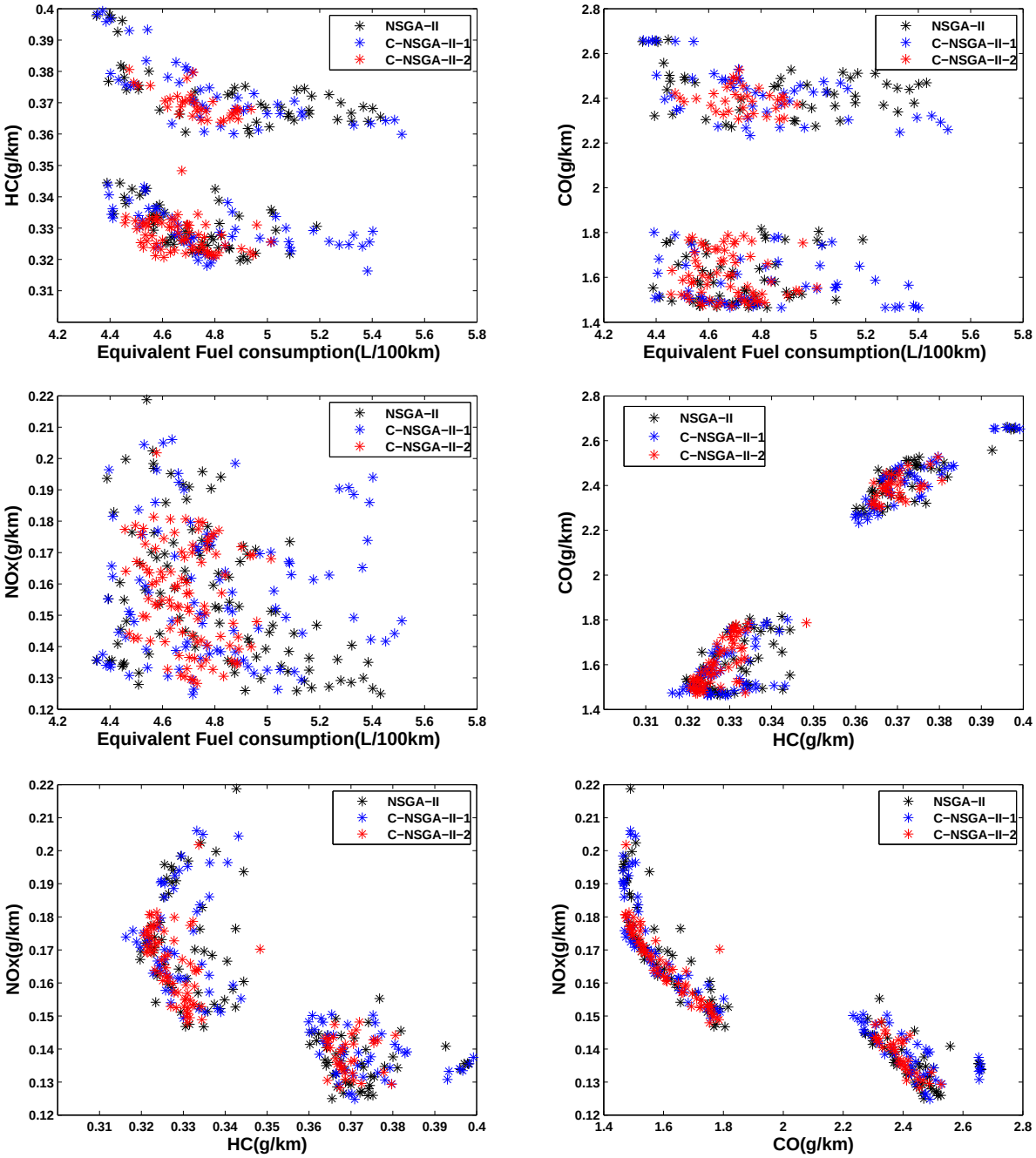

Fig. 11. Simulation results of non-dominated solutions of NSGA-II, C-NSGA-II-1, and C-NSGA-II-2 (a) EFC-HC, (b) EFC-CO, (c) EFC-NOx, (d) HC-CO, (e) HC-NOx, (f) CO-NOx

presents the results of six two-objective combinations from these four objectives. As shown in Figs. 11 (a), 11(b), and 11(c), C-NSGA-II-2 can find more concentrate dots especially in EFC axis at the same emission level than NSGA-II and C-NSGA-II-1, while the other two have much scattered dots which have higher values in the EFC axis. In Fig. 11(d), HC and CO have similar variable trends: when the solution has a small HC value, the CO value is also small. In contrast, as shown in Figs. 11(e) and 11(f), NOx value changes in an opposite trend from HC and CO. Thus, when one solution outperforms in one or two objects, it may have poor performances in other objects. This phe-

nomenon can also be observed in the top of Figs.11 (a) and 11(b), the dots which have the best EFC values perform poorly in the HC axis. Similarly, as shown in Figs. 11(e) and 11(f), the dots which have the best HC or CO values present worse values in NOx axis. This finding indicates that the four objectives are conflicting in some cases, and a solution with all four minimum objective values cannot be found.

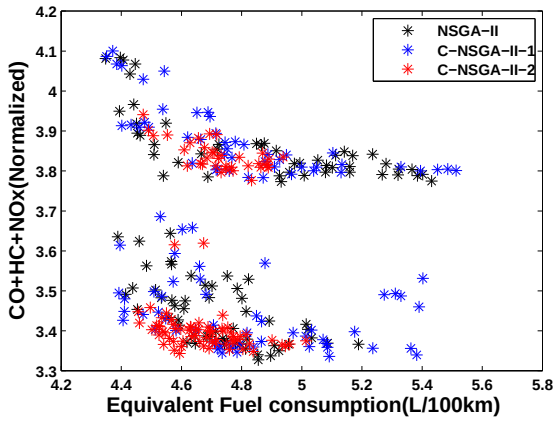

Fig. 12. Simulation results of non-dominated solutions of NSGA-II, C-NSGA-II-1, and C-NSGA-II-2 with EFC and normalized emissions

As shown in Fig. 12, the three emission values are normalized based on the minimum emission values found. Together, the solutions of the three algorithms are presented. C-NSGA-II-2 can obviously find better and more concentrated solutions than the other two. However, determining which between NSGA-II and C-NSGA-II-1 performs better based only on this figure is difficult. Table 4 presents a comparison of these three algorithms' performance by using two metrics. Larger coverage value of C (B,A) than C (A,B) means C-NSGA-II-1 has more solutions, which dominate the ones in NSGA-II than converse. This result means that the additional chaotic initialization, crossover, and mutation operators can improve the performance of the original NSGA-II. C-NSGA-II-2 outperforms both NSGA-II and C-NSGA-II-1 on C metric, which indicates that chaotic disturbance and local search operators can enhance searching ability for better solutions. On the other hand, a smaller spacing metric means better solution distribution. The results in Table 4 show that C-NSGA-II-1 performs best in the solution's distribution. All results are averaged over 10 runs.

C-NSGA-II-2 can find a series of Pareto trade-off solutions. Therefore, vehicle control engineers can use their own criteria to select a solution that meets their goals. The

Table 4. Comparison among NSGA-II, C-NSGA-II-1, and C-NSGA-II-2

Algorithms	**Coverage of two sets (*C*)**	**Spacing (*S*)**
NSGA-II (A)	C (A,B) = 0.832 C (A,C) = 0.735	0.0275
C-NSGA-II-1 (B)	**C (B,A) = 0.902** C (B,C) = 0.778	**0.0221**
C-NSGA-II-2 (C)	**C (C,A) = 0.847** **C (C,B) = 0.873**	0.0282

Table 5. Comparison among four objectives found by the desirable solution and the default solution

Objectives	**Default solution**	**Desirable solution**	**Reduction**
EFC (L/100km)	5.13	4.46	13.07%
HC (g/km)	0.356	0.334	6.29%
CO (g/km)	1.822	1.630	10.52%
NOx (g/km)	0.198	0.164	17.12%

following equation was used to find the desirable solution:

$$G = 0.7 \times \text{FC} + 0.3 \times \text{normalizedEmissions}(\text{HC} + \text{CO} + \text{NOx}) \quad (18)$$

Table 5 shows a comparison of four objective values found by using the desirable solution (obtained by finding minimum G) and the default solution.

As shown in Table 5, the new desirable solution found by C-NSGA-II-2 outperforms the default solution in all four objective values. This result means that if the parameters of this solution are adopted in the HEV controller's design, better performance can be achieved in terms of both EFC and emissions. The MFs of three optimized FLCs from this solution are presented in Fig. 13. The optimal switching speed is $Z21 = 7.5$ (km/h) in this solution.

A comparison between Figs. 13 and 10 indicates that the optimal solution's parameters obtained by using C-NSGA-II-2 are quite different from the default ones. Note that the optimal objects (including fuel economy and emissions) are conflicted with each other; the forms of MFs are changed to regulate the working points of the power components according to the specific optimization criterion. Thus, if the selected criterion is changed, such as the weighting factors of Eq. (17) are changed, another solution could emerge, and the optimal parameters will also change. This finding demonstrates that control engineers can select their desirable solutions from the population of trade-off solutions based on different criteria.

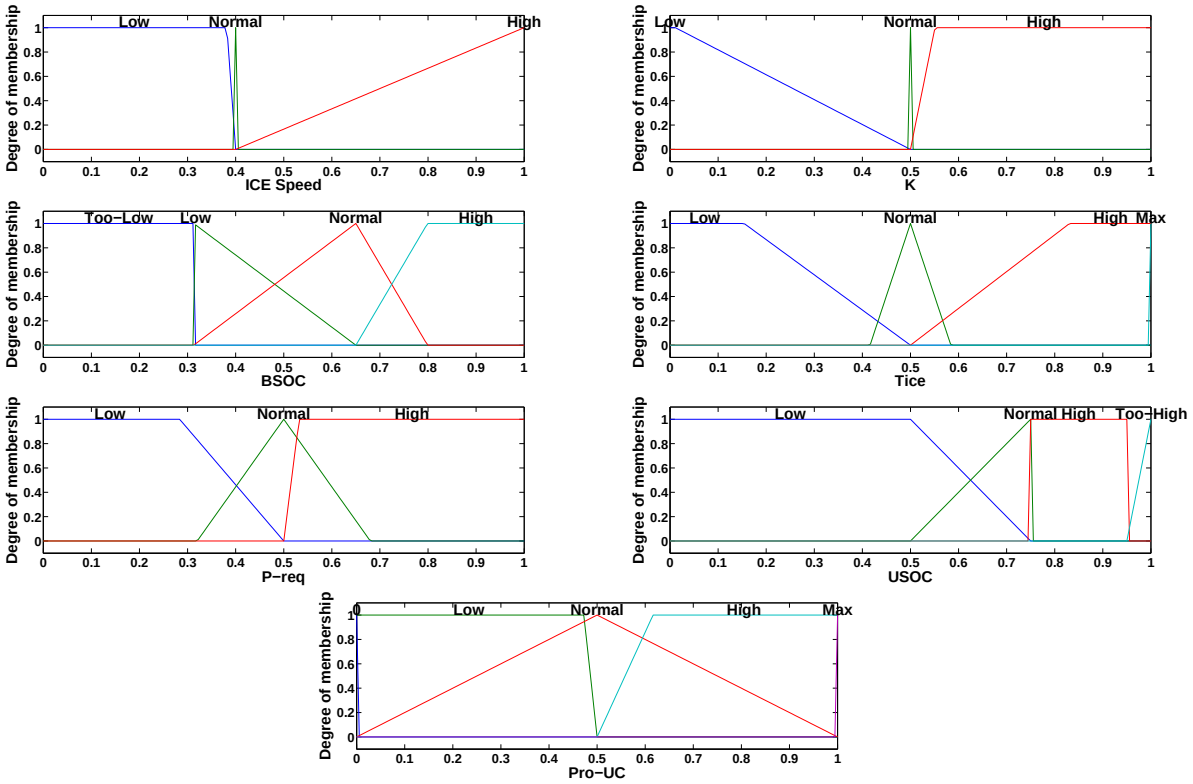

Fig. 13. Membership functions of three optimized FLCs (a) ICE Speed, (b) K, (c) BSOC, (d) Tice, (e) P_req, (f) USOC, and (g) Pro_UC

Simulation results show that chaotic operators can enhance the searching ability of the original NSGA-II, and better solutions can be found by C-NSGA-II. C-NSGA-II can improve the FLCs of target HEV. Therefore, better performance of the target HEV can be expected.

8 CONCLUSION

A fuzzy logic-based EMS is developed for proper management of power distribution in a parallel HEV, which is equipped with a battery/UC-based HESS. Fuzzy system parameters are optimized by using a new genetic algorithm to reduce fuel consumption and three emissions (HC, CO, and NOx) over the ECE driving cycle.

Simultaneously reducing fuel consumption and emissions is a typical multi-objective optimization problem, and many local optima could be present. In this study, chaotic operators, including chaotic initialization, chaotic crossover, chaotic mutation, chaotic disturbance, and chaotic local search, are introduced into NSGA-II. The new algorithm, which is named C-NSGA-II, and the original NSGA-II are adopted in the optimization of fuzzy logic controllers, and their performances are compared. C-NSGA-II-1, which is the first stage of C-NSGA-II, has better searching ability than NSGA-II. Meanwhile, C-NSGA-II-2, which is the second stage of C-NSGA-II, consistently outperforms the first two algorithms. This result indicates that chaotic initialization, chaotic crossover, and mutation operators can enhance the performance of NSGA-II. In addition, chaotic disturbance and local search operators can further improve local searching ability to find better solutions. The ergodicity and pseudo-randomness of chaos can help C-NSGA-II to efficiently address the multi-objective optimization problem in the HEV domain. Adopting C-NSGA-II can create an optimal fuzzy-based EMS, which outperforms the default EMS in terms of fuel consumption and emissions.

Future work will use the tuning process of the fuzzy EMS in different driving cycles, and more optimal results will be obtained. Based on those results, an algorithm that can recognize current driving situations and utilize the optimal results will be developed for an optimal onboard EMS.

REFERENCES

[1] M. Ehsani, Y. Gao, and A. Emadi, Modern Electric, Hybrid Electric, and Fuel Cell Vehicles: CRC Press, 2009.

[2] K. Maeda, H. Fujimoto, and Y. Hori, "Four-wheel Driving-force Distribution Method for Instantaneous or Split Slippery Roads for Electric Vehicle", Automatika-Journal for Control, Measurement, Electronics, Computing and Communications, vol. 2013, no. 54, 2013.

[3] K. Tanoue, H. Yanagihara, and H. Kusumi, "Hybrid is a Key Technology for Future Automobiles Hydrogen Technology". Springer Berlin Heidelberg. pp. 235-272, 2008.

[4] K. Ahn and P.Y. Papalambros, "Engine optimal operation lines for power-split hybrid electric vehicles", Proceedings of the Institution of Mechanical Engineers, Part D: Journal of Automobile Engineering, vol. 2009, no. 223, pp. 1149-1162, 2009.

[5] M. Soleymani, M. Montazeri-Gh, and R. Amiryan, "Adaptive fuzzy controller for vehicle active suspension system based on traffic conditions", Scientia Iranica, vol. 2012, no. 19, pp. 443-453, 2012.

[6] Z. W. Wu, Z. L. Zhang, C. L. Yin, and Z. Zhao, "Design of a soft switching bidirectional DC-DC power converter for ultracapacitor-battery interfaces", International Journal of Automotive Technology, vol. 2012, no. 13, pp. 325-336, 2012.

[7] M.H. Khooban, D. Nazari Maryam Abadi, A. Alfi, and M. Siahi, "Optimal Type-2 Fuzzy Controller For HVAC Systems", Automatika-Journal for Control, Measurement, Electronics, Computing and Communications, vol. 2013, no. 55, 2013.

[8] B. Baumann, G. Rizzoni, and G. Washington, "Intelligent Control of Hybrid Vehicles Using Neural Networks and Fuzzy Logic", vol. 1998, 1998.

[9] N.J. Schouten, M.A. Salman, and N.A. Kheir, "Energy management strategies for parallel hybrid vehicles using fuzzy logic", Control Engineering Practice, vol. 2003, no. 11, pp. 171-177, 2003.

[10] W.W. Xiong, Y. Zhang, and C. Yin, "Optimal energy management for a series–parallel hybrid electric bus", Energy Conversion and Management, vol. 2009, no. 50, pp. 1730-1738, 2009.

[11] J. Solano Martínez, R.I. John, D. Hissel, and M.-C. Péra, "A survey-based type-2 fuzzy logic system for energy management in hybrid electrical vehicles", Information Sciences, vol. 2012, no. 190, pp. 192-207, 2012.

[12] A. Poursamad and M. Montazeri, "Design of genetic-fuzzy control strategy for parallel hybrid electric vehicles", Control Engineering Practice, vol. 2008, no. 16, pp. 861-873, 2008.

[13] L. Chan-Chiao, P. Huei, J.W. Grizzle, and K. Jun-Mo, "Power management strategy for a parallel hybrid electric truck", Control Systems Technology, IEEE Transactions on, vol. 2003, no. 11, pp. 839-849, 2003.

[14] C.Y. Li and G.P. Liu, "Optimal fuzzy power control and management of fuel cell/battery hybrid vehicles", Journal of Power Sources, vol. 2009, no. 192, pp. 525-533, 2009.

[15] H. Borhan, A. Vahidi, A.M. Phillips, M.L. Kuang, I.V. Kolmanovsky, and S. Di Cairano, "MPC-Based Energy Management of a Power-Split Hybrid Electric Vehicle", Control Systems Technology, IEEE Transactions on, vol. 2011, no. 99, pp. 1-11, 2011.

[16] B.Z.Zhang, Z.H. Chen, Mi.C, and Y.L. Murphey, "Multi-objective parameter optimization of a series hybrid electric vehicle using evolutionary algorithms", in Vehicle Power and Propulsion Conference, 2009. VPPC '09. IEEE. pp. 921-925, 2009.

[17] W.W.Xiong, C.L.Yin, Y. Zhang, and J.L. Zhang, "Series-parallel Hybrid Vehicle Control Strategy Design and Optimization Using Real-valued Genetic Algorithm", Chinese Journal Of Mechanical Engineering, vol. 2009, no. 22, 2009.

[18] H.J. Valerie, B.W. Keith, and J.R. David, "HEV Control Strategy for Real-Time Optimization of Fuel Economy and Emissions", SAE Technical Paper 2000-01-1543, vol. 2000, 2000.

[19] X. Hu, Z. Wang, and L. Liao, "Multi-objective optimization of HEV fuel economy and emissions using evolutionary computation", SAE SP, vol. 2004, pp. 117-128, 2004.

[20] K. Deb, A. Pratap, S. Agarwal, and T. Meyarivan, "A fast and elitist multiobjective genetic algorithm: NSGA-II", Evolutionary Computation, IEEE Transactions on, vol. 2002, no. 6, pp. 182-197, 2002.

[21] S. Jeyadevi, S. Baskar, C. Babulal, and M. W. Iruthayarajan, "Solving multiobjective optimal reactive power dispatch using modified NSGA-II", International Journal of Electrical Power & Energy Systems, vol. 2011, no. 33, pp. 219-228, 2011.

[22] H. Lu, R. Niu, J. Liu, and Z. Zhu, "A chaotic non-dominated sorting genetic algorithm for the multi-objective automatic test task scheduling problem", Applied Soft Computing, vol. 2012, 2012.

[23] E. Sciberras and R. Norman, "Multi-objective design of a hybrid propulsion system for marine vessels", Electrical Systems in Transportation, IET, vol. 2012, no. 2, pp. 148-157, 2012.

[24] D. Guo, J. Wang, J. Huang, R. Han, and M. Song, "Chaotic-NSGA-II: an effective algorithm to solve multi-objective optimization problems", in Intelligent computing and integrated systems (ICISS), 2010 international conference on: IEEE. pp. 20-23, 2010.

[25] B.Q. Ren and W.Z. Zhong, "Multi-objective optimization using chaos based PSO", Information Technology Journal, vol. 2011, no. 10, pp. 1908-1916, 2011.

[26] Y.Q. Guo, Y.B. Wu, Z.S. Ju, J. Wang, and L. Y. Zhao, "Remote sensing image classification by the Chaos Genetic Algorithm in monitoring land use changes", Mathematical and Computer Modelling, vol. 2010, no. 51, pp. 1408-1416, 2010.

[27] M. Eslami, H. Shareef, and A. Mohamed, "Power system stabilizer design using hybrid multi-objective particle swarm optimization with chaos", Journal of Central South University of Technology, vol. 2011, no. 18, pp. 1579-1588, 2011.

[28] J.Y. Liang, J.L. Zhang, X. Zhang, S.F. Yuan, and C.L. Yin, "Energy management strategy for a parallel hybrid electric vehicle equipped with a battery/ultracapacitor hybrid energy storage system", Journal of Zhejiang University Science A, vol. 2013, no. 14, pp. 535-553, 2013.

[29] Z.W. Wu, J.L. Zhang, L. Jiang, H.J. Wu, and C.L. Yin, "The energy efficiency evaluation of hybrid energy storage system based on ultra-capacitor and LiFePO4 battery", WSEAS Transactions on Systems, vol. 2012, no. 11, pp. 95-105, 2012.

[30] K. Miettinen, "Some methods for nonlinear multi-objective optimization", in Evolutionary Multi-Criterion Optimization: Springer. pp. 1-20, 2001.

[31] J. Gao and J. Wang, "A hybrid quantum-inspired immune algorithm for multiobjective optimization", Applied Mathematics and Computation, vol. 2011, no. 217, pp. 4754-4770, 2011.

[32] R.M. May, "Simple mathematical models with very complicated dynamics", Nature, vol. 1976, no. 261, pp. 459-467, 1976.

[33] Y. She and C. Shen, "Chaotic search-based adaptive immune genetic algorithm", in Business Intelligence and Financial Engineering, 2009. BIFE'09. International Conference on: IEEE. pp. 74-78, 2009.

[34] R. Storn and K. Price, "Differential evolution–a simple and efficient heuristic for global optimization over continuous spaces", Journal of Global Optimization, vol. 1997, no. 11, pp. 341-359, 1997.

[35] S. Tiwari, "Development and Integration of Geometric and Optimization Algorithms for Packing and Layout Design", PhD thesis, Clemson University. 2009.

[36] S. Kukkonen and J. Lampinen, "GDE3: The third evolution step of generalized differential evolution", in Evolutionary Computation, 2005. The 2005 IEEE Congress on: IEEE. pp. 443-450, 2005.

[37] E. Zitzler, "Evolutionary algorithms for multiobjective optimization: Methods and applications", vol. 63: Shaker Ithaca, 1999.

[38] J.R. Schott, "Fault Tolerant Design Using Single and Multicriteria Genetic Algorithm Optimization", DTIC Document, 1995.

Junyi Liang received the B.S. Degree in Mechanical Engineering from Shanghai Jiao Tong University, Shanghai, China in 2006. He is currently a PhD candidate in Institute of Automotive Engineering, Shanghai Jiao Tong University, China. His research interests include Hybrid Electric Vehicle energy management and hybrid powertrain coordinated transient control.

Jianlong Zhang received the B.S. Degree in Vehicle Engineering from Nanjing University of Science and Technology, Nanjing, China in 1986. He received the M.Sc degree in Vehicle Engineering from Henan University of Science and Technology, Luoyang, China in 2003. He received the Ph.D. degree in Vehicle Engineering from Shanghai Jiao Tong University, Shanghai, China in 2009. He is currently an Assistant research fellow in Institute of Automotive Engineering, Shanghai Jiao Tong University, China. His research interests include Automotive Electronic control, Hybrid Electric Vehicle research and development.

Hu Zhang received the B.S. Degree in Vehicle Engineering from Jilin University, Changchun, China in 2008. He is currently a Ph.D. candidate in National Engineering Laboratory for Automotive Electronic Control Technology at Shanghai Jiao Tong University, Shanghai, China.His research interests include control system design for hybrid electric vehicles and engine management system.

Chengliang Yin received the B.S. Degree in Solid Mechanics from Huazhong University of Technology, Wuhan, China in 1986. He received the M.Sc degree and Ph.D degree in Vehicle Engineering from Jilin Industrial University, Changchun, China in 1996 and 2000. He is currently the vice president and professor of Institute of Automotive Engineering, Shanghai Jiao Tong University, China. His research interests include hybrid electric vehicle and pure electric vehicle technology, automotive Electronic Control technology, transmission technology for hybrid electric vehicle, battery management system and hybrid energy storage system.

AUTHORS' ADDRESSES

Junyi Liang, B.Sc.,
Jianlong Zhang, Ph.D.,
Hu Zhang, B.Sc.,
Prof. Chengliang Yin, Ph.D.,
National Engineering Laboratory for Automotive Electronic Control Technology,
Shanghai Jiao Tong University,
Shanghai, China,
email: Junyi.LiangSH@gmail.com,
zjlong@sjtu.edu.cn,
huzhang0210@gmail.com,
clyin1965@sjtu.edu.cn

Received: 2013-12-17
Accepted: 2014-10-11